Mater Renew Sustain Energy (2015)4:18
DOI 10.1007/s40243-015-0060-y

ORIGINAL PAPER

One-step synthesis of composite thin film with ZnSe and PbTeSe ternary solid solution

Seishi Abe[1]

Received: 7 January 2015 / Accepted: 16 September 2015

Abstract This study investigates one-step synthesis of composite thin film with ZnSe and PbTeSe ternary solid solution using hot-wall deposition (HWD) with multiple resources of PbTe and ZnSe. HWD consists of three electric furnaces, designated as wall, source-1, and source-2. The PbTe and ZnSe sources were located in the source-2 and source-1 furnaces for simultaneous evaporation to a glass substrate (Corning Eagle 2000). The substrate temperature was changed by circulating water controlled at temperatures of 340–274 K. X-ray diffraction indicates that composite thin films contain ZnSe with zinc-blende structure and PbTeSe ternary solid solution with NaCl structure. The Raman spectrum also suggests formation of ZnSe without alloying with Pb or Te. The lattice constant of the ternary solid solution gradually increases with increasing source temperature of PbTe. High-resolution transmission electron microscopy indicates that the ternary solid solution forms isolated nanocrystals of 16–30 nm in the composite thin film. Therefore, composite thin films are composed of PbTeSe ternary solid solution nanocrystals embedded in a ZnSe matrix.

Keywords Semiconductor nanocrystal · Hot-wall deposition · X-ray diffraction · High-resolution TEM

Introduction

Composite thin film with semiconductor nanocrystals embedded in a matrix has a potential application for quantum dot solar cells [1]. Semiconductor nanocrystals provide a shift in optical absorption edge due to quantum size effects, capable of tuning an optical gap to effective energy region for absorbing visible and near infrared light in solar radiation spectrum [2–9].

We proposed a composite thin film with PbSe nanocrystals embedded in a ZnSe matrix by one-step synthesis using hot-wall deposition (HWD) with multiple evaporation sources of PbSe and ZnSe [10]. In the PbSe-ZnSe system in thermal equilibrium, the mutual solubility range is quite narrow (less than 1 mol%) at temperatures below 1283 K [11]. Hence, this system phase-separates in a composite and provides compositional steepness at the hetero-interface between PbSe and ZnSe. In addition, a composite thin film of PbSe nanocrystal embedded in a ZnSe matrix is capable of exhibiting quantum size effects because of the relatively large exciton Bohr radius of 46 nm in PbSe [12] and the relatively larger band gap difference between ZnSe (2.67 eV) [13] and PbSe (0.27 eV) [14]. Elemental mapping indicated that isolated PbSe nanocrystals are dispersed in the ZnSe matrix [10]. The optical absorption edge shifts toward the lower-photon-energy region as PbSe content increases. Thus, the insoluble material system and HWD enable a one-step synthesis of PbSe-ZnSe composite thin film. In the next step, ternary solid solution $PbTe_{1-x}Se_x$ seems to be effective for nanocrystal due to potential modifications in the properties (e.g., energy band gap, carrier concentration, and low temperature stability) of nanocrystal. In particular, crystallization of quantum dots at room temperature is valuable for a low-cost product for such use. In the present

✉ Seishi Abe
abe@denjiken.ne.jp

[1] Research Institute for Electromagnetic Materials, 2-1-1 Yagiyama-minami, Sendai 982-0807, Japan

Published online: 25 September 2015

study, one-step synthesis of composite thin film with ZnSe and $PbTe_{1-x}Se_x$ ternary solid solution is investigated.

Experimental

Composite thin film was prepared using HWD. Figure 1 is a schematic diagram of the HWD apparatus used. It consists of three electric furnaces, designated as wall, source-1, and source-2. The temperature of each could be controlled independently. The substrate temperature was changed by circulating water controlled at temperatures of 340–274 K. With HWD, deposition and re-evaporation are continuously repeated on the film surface, resulting in a state of near thermal equilibrium [15]. PbTe and ZnSe were used as evaporation sources with 5 N purity. The PbTe and ZnSe sources were located in the source-2 and source-1 furnaces for simultaneous evaporation to a glass substrate (Corning Eagle 2000). Here, the temperatures were kept constant at 683 K for the wall, and 843 K for source-1 (ZnSe). The source-2 (PbTe) temperature was varied from 753 K to 793 K to provide different PbTe concentrations. The composite thin film was structurally characterized using X-ray diffraction (XRD) with Cu Kα radiation (Rigaku RAD-X, Tokyo, Japan). A symmetric $2\theta-\theta$ configuration was used. The composition of the film was analyzed using energy dispersive spectroscopy (EDS) (EDAX model, Phoenix, NJ, USA) operating at 10 kV with standard samples of PbTe to calibrate the analyzed results for Pb and Te and with ZnSe for Zn and Se. The film was directly observed using transmission electron microscopy (TEM) operating at 300 kV (Hitachi H-9000NAR, Tokyo, Japan). Ion milling was performed in the sample preparation. The Raman spectrum of the film was measured using a Raman spectrometer (JASCO NRS-5000, Tokyo, Japan) with a pumping semiconductor laser at 532 nm.

Results and discussion

Figure 2 depicts the EDS analysis results of the composite thin films with respect to the source temperature of PbTe. The concentration of Pb increases monotonically with increasing source temperature, while element Te can be detected at relatively high temperatures (exceeding 788 K). The EDS apparatus used is capable of detecting Te concentrations exceeding 1at.%. Hence, the composite thin films contain relatively low concentrations of Te, despite the use of evaporation source PbTe. The composition ratio of anion with Se and Te to cation with Zn and Pb is depicted in the inset. The composition ratio is found to be a slight anion-deficit deviation from stoichiometry, probably due to the small inclusion of Te.

Figure 3 depicts the XRD pattern of the composite thin films as a function of the source temperature of PbTe. In this case, the substrate temperature is kept constant at 340 K. A phase mixture with zinc-blende structure and NaCl structure (NaCl-I) is first observed at 753 K, and a different phase with NaCl structure (NaCl-II) appears at 793 K. Hence, the phase with NaCl structure changes from NaCl-I to a phase mixture of NaCl-I and NaCl-II with respect to the source temperature, while remaining a phase with zinc-blende structure regardless of temperature.

Figure 4 depicts the lattice constant of the composite thin films as a function of the source temperature of PbTe. The lattice constant is estimated from the XRD peak at

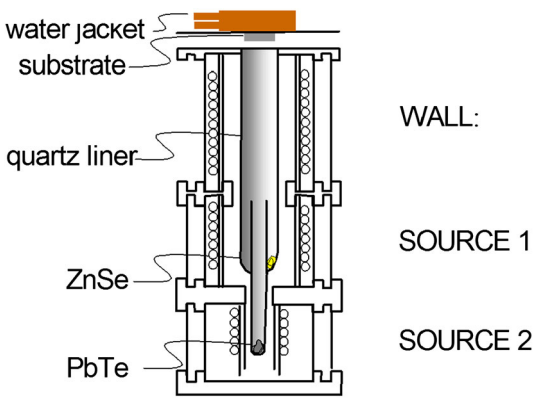

Fig. 1 The HWD apparatus used in the study consists of three electric furnaces: wall, source-1 for ZnSe, and source-2 for PbTe. The substrate temperature is changed by circulating water controlled at temperatures of 340 K to 274 K

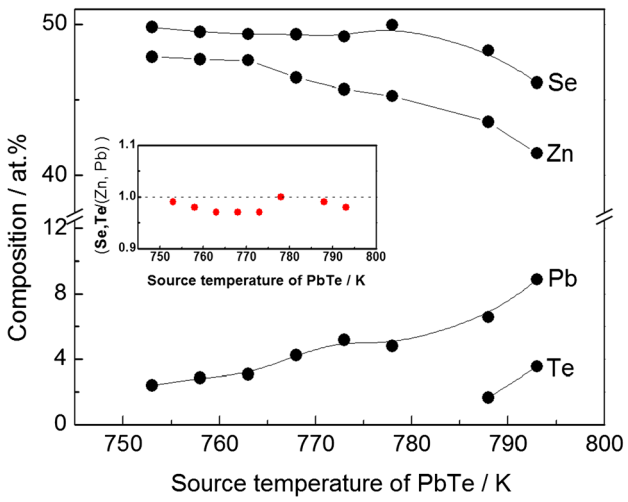

Fig. 2 Results of EDS analysis of composite thin films prepared at the substrate temperature of 340 K as a function of the source temperature of PbTe. Inset indicates the composition ratio of anion with Se and Te to cation with Zn and Pb

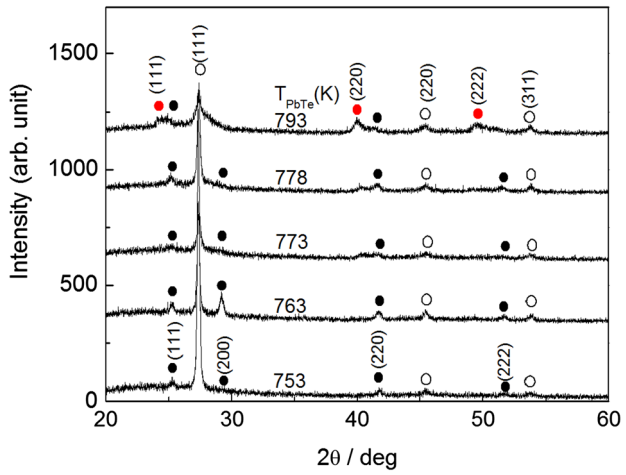

Fig. 3 XRD pattern of composite thin films prepared at the substrate temperature of 340 K with respect to the source temperature of PbTe. *Black circle* indicates a phase with NaCl structure (NaCl-I), *red circles* indicate a different phase with NaCl structure (NaCl-II), and *circles* indicate a phase with zinc-blende structure

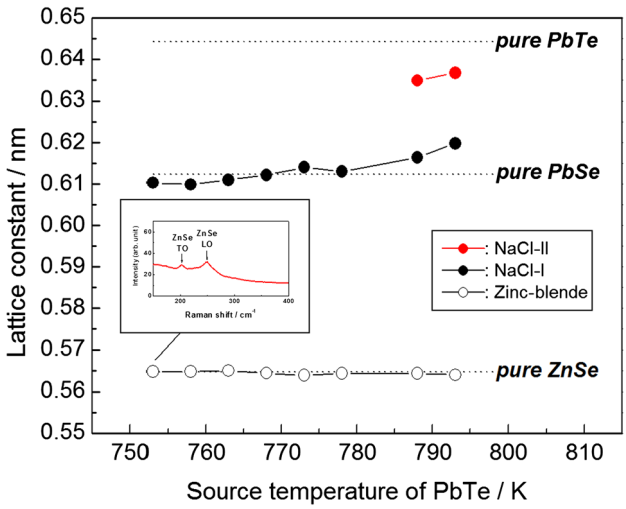

Fig. 4 Lattice constant of composite thin films prepared at the substrate temperature of 340 K as a function of the source temperature of PbTe. Inset indicates the Raman spectrum of composite thin film at the source temperature of 753 K

(111) Bragg reflection for zinc-blende structure and the peak at (220) for NaCl-I and NaCl-II with relatively strong intensity (Fig. 3). The broken lines indicate the lattice constant of standard ZnSe, PbSe, and PbTe. The lattice constant for zinc-blende structure is almost the same as that of ZnSe. If a solid solution is formed in ZnSe with elements Te and Pb, the lattice constant should increase with increasing source temperature of PbTe, due to the difference in radii between Te and Se or Pb and Zn. In addition, the PbSe-ZnSe system and PbTe-ZnTe system phase-separate in thermal equilibrium [16]. Furthermore, the inset depicts the Raman spectrum of the composite at the source temperature of 753 K. The peaks at 203 and 250 cm^{-1} are attributed to transverse optical phonon mode and longitudinal optical phonon mode in ZnSe [17]. Therefore, the phase with zinc-blende structure is reasonably assigned to ZnSe, regardless of the source temperature of PbTe. In NaCl-I, the lattice constant is close to that of PbSe and gradually increases with increasing source temperature of PbTe. In NaCl-II, the lattice constant is larger than that of NaCl-I and tends to increase as the temperature increases. Hence, the two phases NaCl-I and NaCl-II seem to form a solid solution of $PbTe_{1-x}Se_x$ with different compositions x.

Here, we investigate precisely why the lattice constant of NaCl-I is close to that of PbSe despite the use of an evaporation-source PbTe. In thermal equilibrium between the solid state and the vapor state, PbTe forms dominantly a binary compound in vapor state with species of 98 % [18] [$PbTe(s) = PbTe(g)$], while ZnSe dissociates to each element [19] [$ZnSe(s) = Zn(g) + 1/2Se_2(g)$]. Hence, the vapor phase contains mainly three species (PbTe, Zn, and Se) in which PbTe and Se are chemically in equilibrium with PbSe and Te [20]: $PbTe(g) + 1/2Se_2(g) = PbSe(g) + 1/2Te_2(g)$. This reaction results in ternary solid solution $PbTe_{1-x}Se_x$ in solid state [20]. Evaporation sources PbTe and ZnSe may produce ZnSe and $PbTe_{1-x}Se_x$ in solid state and residual Te in the vapor state as $PbTe(g) + Zn(g) + (1+x)/2Se_2(g) \rightarrow ZnSe(s) + PbTe_{1-x}Se_x(s) + x/2Te_2(g)$. Most of the residual Te in the vapor state is probably exhausted, since composition analysis indicates a small inclusion of Te with anion-deficit deviation from stoichiometry (Fig. 2). Therefore, evaporation sources PbTe and ZnSe should produce dominantly a phase mixture of ZnSe and solid solution $PbTe_{1-x}Se_x$, in which composition x is controlled by the partial pressure of Se dissociated from evaporation source ZnSe. NaCl-I is expected to have a composition close to $x = 1$ at relatively low temperatures (below 788 K), since their lattice constants are close to that of standard PbSe (Fig. 4). This composition indicates that a sublimated amount of Se is almost twice as large as that of PbTe, according to the above reaction. In this case, the reaction process should be limited by sublimation of the ZnSe source.

In quantitative evaluation, composition x in $PbTe_{1-x}Se_x$ can be expressed by partial pressures of PbTe (P_{PbTe}) and PbSe (P_{PbSe}) as [20] $x = P_{PbSe}/(P_{PbTe} + P_{PbSe})$. Partial pressure P can also be expressed using the Clausius–Clapeyron equation [20] $P = P_0 \exp(\Delta H_s/RT)$, where P_0 is the saturation vapor pressure, ΔH_s is the heat of sublimation, R is a gas constant, and T is the temperature. The following equation can be derived from the above equation:

$$\log\left(\frac{1-x}{x}\right) = \log\frac{P_{0\,(\mathrm{PbTe})}}{P_{0\,(\mathrm{PbSe})}} + \frac{\Delta H_{\mathrm{S}\,(\mathrm{PbSe})}}{RT_{\mathrm{PbSe}}} - \frac{\Delta H_{\mathrm{s}\,(\mathrm{PbTe})}}{RT_{\mathrm{PbTe}}}.$$

In this equation, the parameter related to Se (T_{PbSe}) is limited by the source temperature of ZnSe, kept constant at 843 K. Hence, concentration x can be changed only with respect to the source temperature of PbTe (T_{PbTe}).

Figure 5 depicts the temperature dependence of composition x in NaCl-I and NaCl-II. Composition x is estimated from the lattice constants of NaCl-I and NaCl-II at (220) reflection (Fig. 2), assuming linear variation of the lattice constant between PbTe and PbSe following Vegard's law. Here, the smallest lattice constant at 758 K for NaCl-I should be regarded as that of PbSe (Fig. 4) to avoid a numerically negative composition x. The composition $1-x/x$ in NaCl-I exhibits linear variation with respect to the inverse temperature of the PbTe source, indicating that NaCl-I forms a solid solution of $PbTe_{1-x}Se_x$ even at relatively low temperatures below 788 K, with no detection of Te in EDS analysis (Fig. 2). The activation energy is estimated to be 404 kJ/mol, which is close to that of the heat of sublimation in ZnSe (392 kJ/mol) [21]. Therefore, sublimation in ZnSe source actually dominates the reaction in the vapor state to produce $PbTe_{1-x}Se_x$ ternary solid solution with relatively high composition x. In NaCl-II, experiment results at a different substrate temperature (330 K) are added to estimate activation energy, due to difficulty in estimation with only two plots at 340 K (Fig. 4). Activation energy in NaCl-II is also estimated to be 263 kJ/mol, which is near that of the heat of sublimation in PbTe (224 kJ/mol) [22]. Hence, sublimation in PbTe source nearly dominates the reaction to produce a solid solution with relatively small composition x. Consequently, evaporation sources PbTe and ZnSe provide a phase mixture of ZnSe and ternary solid solution $PbTe_{1-x}Se_x$.

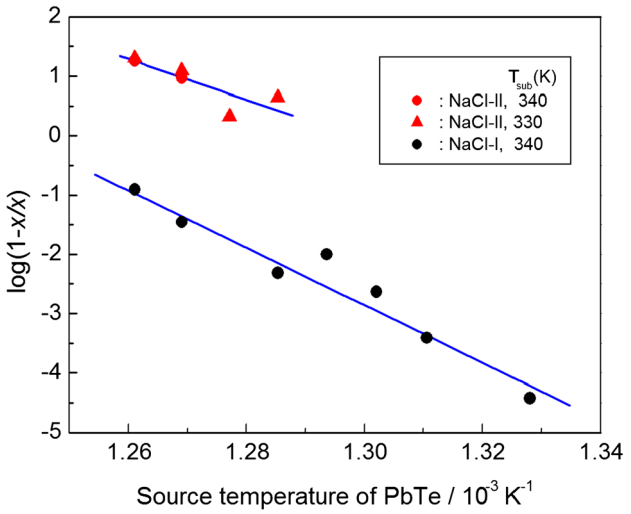

Fig. 5 Temperature dependence of composition x in NaCl-I and NaCl-II

Next, temperature dependence of the substrate is investigated for NaCl-I to clarify whether a slight inclusion of Te modifies low temperature stability in the crystalline state of PbSe. Figure 6a depicts the XRD pattern of composite thin films with respect to substrate temperature. In this case, Pb concentration in the composite film is kept constant at 3.5 ± 0.5at.%. Hence, the films are expected to contain 7at.%$PbTe_{1-x}Se_x$ ternary solid solution with relatively large composition x. For example, composition x is estimated to be 0.968 at 340 K from the diffraction peak. The diffraction peak in ZnSe with zinc-blende structure clearly crystallizes even at a substrate temperature of 274 K. The dotted area is enlarged in Fig. 6b for easier viewing. The dotted line indicates the peak position of the standard PbSe. The diffraction peak of NaCl-I is also close to that of PbSe and becomes weak as the substrate temperature decreases. Typical mean grain size is estimated to be 22 nm at 340 K from the full width at half maximum of the diffraction peak, according to Scherrer's formula [23].

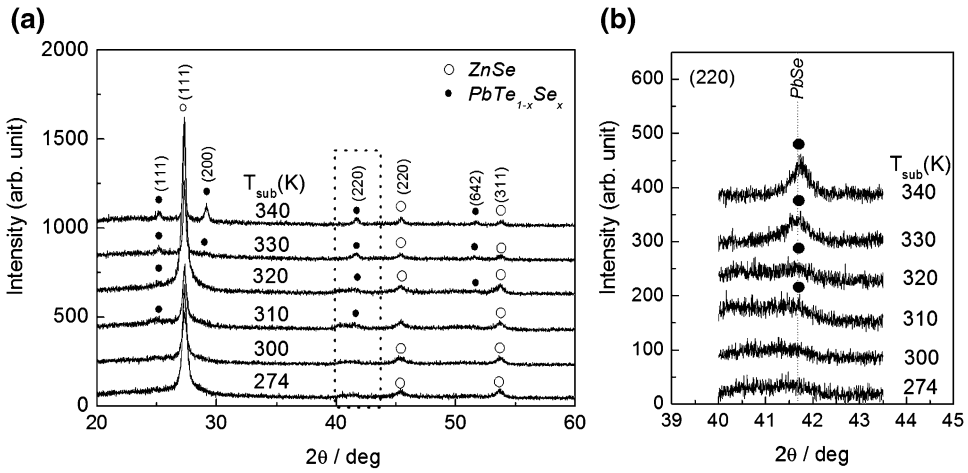

Fig. 6 XRD pattern of composite thin films with respect to substrate temperature. **a** 2θ range from 20 to 60 deg. *Black circles* denote NaCl-I, and *white circles* denote ZnSe with zinc-blende structure. **b** Enlarged image for easier viewing. The *dotted line* indicates the peak position of standard PbSe

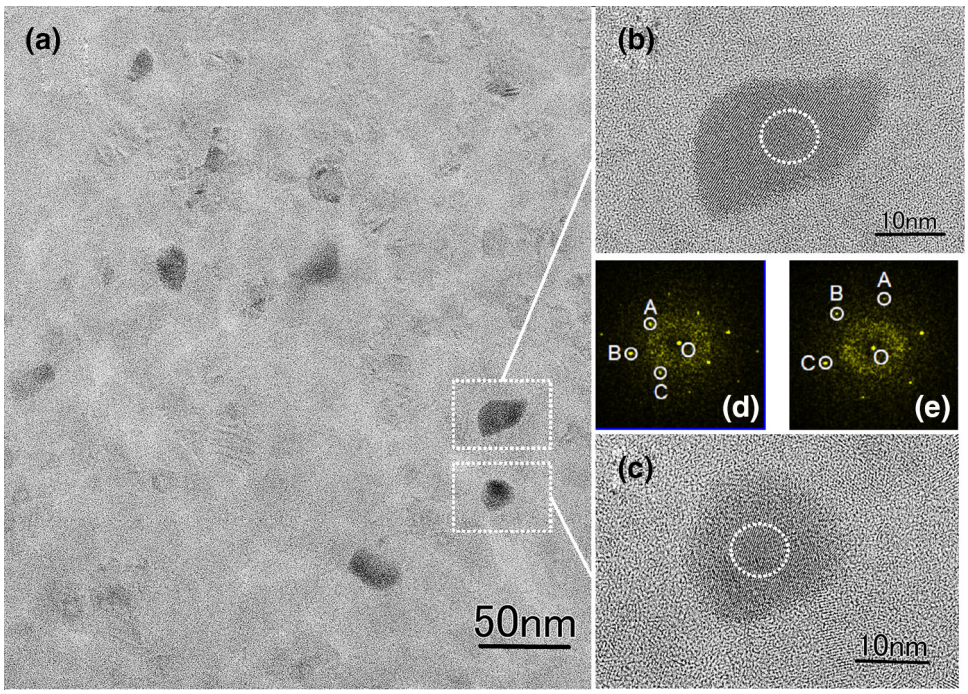

Fig. 7 Direct observation of composite thin film prepared at the substrate temperature of 274 K. **a** TEM image. **b** and **c** High-resolution EM images of the dotted areas in Fig. 7a. **d** and **e** FFT diffraction patterns of the selected areas denoted by circles in Fig. 7b, c

It is unclear whether the phase crystallizes at 274 K, due to a weak diffraction peak. TEM observation of the composite film at 274 K is performed next.

Figure 7a presents a TEM image of the composite thin film at a substrate temperature of 274 K. Slightly dark isolated particles of 15–30 nm are dispersed in the sample. Figures 7b and c present at high-resolution TEM image of the two typical dotted areas in Fig. 7a. A lattice fringe is clearly observed in the two sphere-like particles in Figs. 7b and c. Fast Fourier transform (FFT) analysis determines the details of the local structure in the nanocrystals. Figure 7d and e depicts the corresponding FFT diffraction patterns of the nanocrystal, denoted by circles in Figs. 7b, c. Both diffraction patterns can be indexed to cubic PbSe. In Fig. 7d, the spots labeled A, B, and C correspond to crystal faces of (200), (220), and (020) in the cubic PbSe, with plane widths of 0.309, 0.219, and 0.307 nm. The angles labeled A-O-B, A-O-C, and B-O-C are 45°, 90°, and 45°. The standard data indicate a plane width of 0.306 nm at both (200) and (020), and 0.217 nm at (220), with an angle of 45 deg for both A-O-B and B-O-C and 90 deg for A-O-C. The lattice alignment of the nanocrystal is close to that of bulk PbSe observed along the [111] direction In Fig. 7e, the spots labeled A, B, and C correspond to crystal faces of (02-2), (20-2), and (2-20) in the cubic PbSe, with plane widths of 0.221, 0.220, and 0.220 nm. The angles labeled A-O-B, A-O-C, and B-O-C are 59°, 119°, and 60°. The standard data (JCPDS 06-0354) indicate a plane width of 0.217 nm at (02-2), (20-2), and (2-20), with an angle of 60° for both A-O-B and B-O-C and 120° for A-O-C. The lattice alignment of the nanocrystal corresponds to that of bulk PbSe observed along the [100] direction. These analysis results are close to the standard PbSe. Furthermore, all the plane widths estimated from FFT analysis are slightly larger than those in standard PbSe, suggesting a slight inclusion of Te in PbSe, with no detection in our EDS analysis. The observed nanocrystal is thus found to be the ternary solid solution NaCl-I. It should be noted that the $PbTe_{1-x}Se_x$ thus observed crystallizes even at 274 K, while the XRD peak of PbSe in the PbSe-ZnSe composite thin films is weak even at the relatively high temperature of 403 K [24]. In contrast, PbTe crystallizes even at 274 K in PbTe-ZnTe composite thin films in our preliminary experiment. These results suggest that the slight inclusion of Te in PbSe stabilizes a crystalline state at a relatively low substrate temperature. Figure 8 depicts the optical absorption spectrum of the composite thin film prepared at 274 K. For comparison, the optical absorption spectrum of pure ZnSe thin film is also presented. The absorption edge in pure ZnSe appears at relatively high photon energy (2.65 eV), while the composite film exhibits broad absorption with onset absorption at 1 eV, due to the presence of PbTeSe nanocrystals embedded in the ZnSe matrix.

One-step synthesis provides a nanocomposite thin film with $PbTe_{1-x}Se_x$ nanocrystals embedded in the ZnSe matrix during phase transformation from PbTe to ternary solid solution with a slight inclusion of Te (NaCl-I). In the composite, ZnSe is the most thermodynamically stable among lead- and zinc-chalcogenides with he lowest free energy of reaction [25]. Hence, it is reasonable for

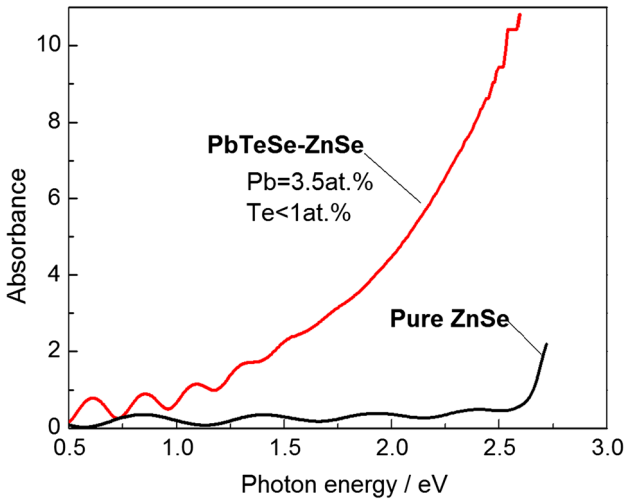

Fig. 8 Optical absorption spectrum of composite thin film prepared at the substrate temperature of 274 K

ZnSe to appear in the production, regardless of the source temperature of PbTe. Thus, the composition in $PbTe_{1-x}Se_x$ nanocrystal can be controlled independently, while the ZnSe matrix remains unchanged. The present result of producing $PbTe_{1-x}Se_x$ additionally suggests similar phase transformation from PbS, which is also in the lead-chalcogenide family, to ternary solid solution $PbS_{1-x}Se_x$. In our preliminary experiment, evaporation sources with PbS and ZnSe provide a composite film with $PbSe_{1-x}S_x$ and ZnSe, indicating that PbS also phase transforms to ternary solid solution $PbS_{1-x}Se_x$ in one-step synthesis.

Conclusions

We investigated one-step synthesis of a composite thin film with $PbTe_{1-x}Se_x$ nanocrystals embedded in a ZnSe matrix during HWD with evaporation sources ZnSe and PbTe. Crystallized ZnSe appears regardless of temperature in the PbTe-source and substrate. Evaporated PbTe transforms to $PbTe_{1-x}Se_x$ ternary solid solution during the reaction between the two sublimated species PbTe and Se, which is dissociated from ZnSe. Se concentration x decreases with increasing source temperature of PbTe. The $PbTe_{1-x}Se_x$ thus obtained crystallizes even at a relatively low substrate temperature of 274 K and disperses in the film as a nanoparticle of 15–30 nm. The ternary solid solution is expected to modify various properties (e.g., energy band gap and carrier concentration). Further investigation is therefore needed on the composite thin film with ZnSe and $PbTe_{1-x}Se_x$ ternary solid solution.

Acknowledgments The present work was supported by a Grant-in-Aid for Scientific Research from the Japan Society for the Promotion of Science (No. 24360295). The author gratefully acknowledges the valuable comments of President T. Masumoto [Research Institute for Electromagnetic Materials (DENJIKEN), Sendai, Japan]. The author is also grateful to Mr. N. Hoshi (DENJIKEN) and Ms. S. Sato (DENJIKEN) for assisting in the experiments.

References

1. Nozik, A.J.: Quantum dot solar cells. Phys. E **14**, 115–120 (2002)
2. Liu, D., Kamat, P.V.: Photoelectrochemical behavior of thin CdSe and coupled TiO_2/CdSe semi-conductor films. J. Phys. Chem. **97**, 10769–10773 (1993)
3. Weller, H.: Quantum sized semiconductor particles in solution in modified layers. Ber. Bunsen-Ges. Phys. Chem. **95**, 1361–1365 (1991)
4. Zhu, G., Su, F., Lv, T., Pan, L., Sun, Z.: Au nanoparticles as interfacial layer for CdS quantum dot-sensitized solar cells. Nanoscale Res. Lett. **5**, 1749–1754 (2010)
5. Hoyer, P., Könenkamp, R.: Photoconduction in porus TiO_2 sensitized by PbS quantum dots. Appl. Phys. Lett. **66**, 349–351 (1995)
6. Chatterjee, S., Goyal, A., Shah, I.: Inorganic nanocomposites for next generation photovoltaics. Mater. Lett. **60**, 3541–3543 (2006)
7. Yang, W., Wan, F., Chen, S., Jiang, C.: Hydrothermal growth and application of ZnO nanowire films with ZnO and TiO_2 buffer layers in dye-sensitized solar cells. Nanoscale Res. Lett. **4**, 1486–1492 (2009)
8. Abe, S., Ohnuma, M., Ping, D.H., Ohnuma, S.: Anatase-dominant matrix in Ge/TiO_2 thin films prepared by RF sputtering method. Appl. Phys. Exp. **1**, 095001 (2008)
9. Abe, S.: InSb-added TiO_2 nanocomposite films by RF sputtering. Nanoscale Res. Lett. **8**, 269 (2013)
10. Abe, S.: One-step synthesis of PbSe-ZnSe composite thin film. Nanoscale Res. Lett. **6**, 324 (2011)
11. Oleinik, G.S., Mizetskii, P.A., Nizkova, A.I.: Nature of the interaction between lead and zinc chalcogenides. Inorg. Mater. **18**, 734–735 (1982)
12. Wise, F.W.: Lead salts quantum dots the limit of strong confinement. Acc. Chem. Res. **33**, 773–780 (2000)
13. Adachi, S., Taguchi, T.: Optical properties of ZnSe. Phys. Rev. B **43**, 9569–9577 (1991)
14. Zemel, J.N., Jensen, J.D., Schoolar, R.B.: Electrical and optical properties of epitaxial films of PbS, PbSe, PbTe, and SnTe. Phys. Rev. **140**, A330–A342 (1965)
15. Lopez-Otero, A.: Hot wall epitaxy. Thin Solid Films **49**, 3–57 (1978)
16. Grytsiv, V.I., Tomashik, V.N., Olejnik, G.C., Tomashik, Z.F.: Investigation of the ZnTe-PbTe system [in Russian]. Izv. AN. SSSR. Neorg. Mater. **16**, 543 (1980)
17. Wang, H.I., Tang, W.T., Liao, L.W., Tseng, P.S., Luo, C.W., Yang, C.S., Kobayashi, T.: Femtosecond laser-induced formation of Wurtzite phase ZnSe nanoparticles in air. J. Nanomater. **012**, 278364 (2012)
18. Brebrick, R.F., Straus, A.J.: Partial pressures in equilibrium with group IV tellurides. I. Optical absorption method and results for PbTe. J. Chem. Phys. **40**, 3230 (1964)

19. Goldfinger, P., Jeunehomme, N.: Mass spectrometric and Knudsen-cell vaporization studies of group 2B-6B compounds. Trans. Fraday Soc. **59**, 2851 (1963)
20. Moritz, T., Schafer, P.: Preparation of Pb(Te,Se) films by simultaneous evaporation of PbTe and Se. Phys. Stat. Sol. (a) **89**, Kl19 (1985)
21. Boev, E.I., Benderskii, L.A., Mil'kov, G.A.: Thermal dissociation of zinc group chalcogenides. 1. Thermal dissociation of zinc sulphide and selenide. Russ. J. Phys. Chem. **43**, 776 (1969)
22. Mills, K.C.: Thermodynamic Data for Inorganic Sulphide Selenides and Tellurides. Butterworth, London (1974)
23. Guinier, A.: X-ray diffraction in crystals, imperfect crystals, and amorphous bodies. Dover Publications, New York (1994)
24. Oba, Y., Abe, S., Ohnuma, M., Sato, N., Sugiyama, M.: Temperature dependence of nanostructure in PbSe–ZnSe composite thin film. J. Phys. D Appl. Phys. **47**, 435102 (2014)
25. Kubaschewski, O., Alock, C.B.: Metallurgical Thermochemistry, vol. 286, 5th edn. Pergamon Press, Oxford (1979)